The PX domains of p47phox and p40phox bind to lipid products of PI(3)K

Fumihiko Kanai*†, Hui Liu*†, Seth J. Field†,‡,§, Hares Akbary*†, Tsuyoshi Matsuo‡, Glenn E. Brown*¶, Lewis C. Cantley‡ and Michael B. Yaffe*¶#

*Center for Cancer Research and Department of Biology, Massachusetts Institute of Technology, Cambridge, Massachusetts 02139, USA
‡Division of Signal Transduction, Beth Israel Deaconess Medical Center, and Department of Cell Biology, Harvard Medical School, Boston, Massachusetts 02215, USA
§Division of Endocrinology, Massachusetts General Hospital, Boston, Massachusetts 02114 USA
¶Department of Surgery, Beth Israel Deaconess Medical Center, Boston, Massachusetts 02215, USA
†These authors contributed equally to this work.
#e-mail: myaffe@mit.edu

PX domains are found in a variety of proteins that associate with cell membranes, but their molecular function has remained obscure. We show here that the PX domains in p47phox and p40phox subunits of the phagocyte NADPH oxidase bind to phosphatidylinositol-3,4-bisphosphate (PtdIns(3,4)P_2) and phosphatidylinositol-3-phosphate (PtdIns(3)P), respectively. We also show that an Arg-to-Gln mutation in the PX domain of p47phox, which is found in patients with chronic granulomatous disease, eliminates phosphoinositide binding, as does the analogous mutation in the PX domain of p40phox. The PX domain of p40phox localizes specifically to PtdIns(3)P-enriched early endosomes, and this localization is disrupted by inhibition of phosphoinositide-3-OH kinase (PI(3)K) or by the Arg-to-Gln point mutation. These findings provide a molecular foundation to understand the role of PI(3)K in regulating neutrophil function and inflammation, and to identify PX domains as specific phosphoinositide-binding modules involved in signal transduction events in eukaryotic cells.

PX domains, named for their presence in the p40phox and p47phox subunits of the NADPH oxidase[1], are ~140-amino-acid-long modules found in more than 150 eukaryotic proteins, including 45 proteins in humans. In addition to the subunits of the neutrophil NADPH oxidase, PX domains are found in other proteins involved in neutrophil function, such as phospholipase D1 and D2, a number of proteins involved in vesicular trafficking, including 15 sorting nexins in humans (SNX1–SNX15)[2–4], and the vacuolar sorting/morphogenesis proteins Vps5p, Vps17p (ref. 5), Vam7p (ref. 6), and Mvp1p (ref. 7) in *Saccharomyces cerevesiae*. Furthermore, PX domains are found in bud-emergence proteins, Bem1p and Bem3p, the protein kinase CISK involved in cell survival[8], and several proteins of unknown function.

The role of the PX domains in subunits of the NADPH oxidase has been obscure. In neutrophils and other phagocytic cells, this enzyme catalyses the production of superoxide as a starting material for the oxidant-mediated killing of invading microorganisms[9,10]. In unstimulated cells, the oxidase is maintained in an inactive state by partitioning the components into a cytoplasmic fraction containing p40phox, p47phox and p67phox, and a membrane-bound flavocytochrome that contains p22phox and gp91phox. The cytoplasmic phox components exist as a complex with a relative molecular mass of ~250,000 (M_r 250K), which is stabilized through multiple SH3-domain-mediated interactions, whereas the membrane-bound components appear to be located primarily on secretory vesicles and specific granules[9,10]. After stimulation and phagocytosis, the cytoplasmic subunits (primarily p47phox) become extensively phosphorylated, and the entire cytoplasmic complex, along with the small G-protein Rac, translocates to the plasma membrane[11], presumably at sites of the developing phagosome. Vesicles containing the membrane-bound components fuse with the phagosome and the plasma membrane, forming an active enzyme complex capable of producing toxic O_2^- in a respiratory burst of oxygen consumption. Human mutations that cause loss or inactivation of p47phox, p67phox, p22phox or gp91phox are responsible for inherited chronic granulomatous disease, which is characterized by an inability to generate superoxide, a marked susceptibility to bacterial and fungal infections, and a shortened lifespan[12].

Multiple lines of evidence from many investigators have implicated specific 3-phosphoinositol lipids in these processes. PtdIns(3,4,5)P_3 is rapidly produced upon neutrophil activation, and Wortmannin, a specific inhibitor of PI(3)K, completely blocks the oxidative burst[13–15]. Furthermore, neutrophils from mice that lack the p110γ form of PI(3)K cannot produce PtdIns(3,4,5)P_3, and display impaired respiratory burst activity[16]. However, the link between these phospholipids and neutrophil function has remained mysterious.

An examination of the sequence alignment of multiple PX domains revealed conserved regions containing basic and hydrophobic amino acids that are reminiscent of the sequence characteristics of domains known to bind to specific phosphopeptides[17] or phospholipids[18] (Fig. 1). Given the known role of PI(3)K in signal-transduction pathways, which involve many of these proteins, we tested whether the p40phox or p47phox PX domains would bind to specific phosphoinositides. We constructed glutathione *S*-transferase (GST)-fusion proteins that contain these PX domains (see Supplementary Information, Fig. S1), and tested their ability to bind to specific phosphoinositides by using a lipid-binding assay[19] (Fig. 2). The PX domain from p47phox bound strongly to PtdIns(3,4)P_2, and more weakly to PtdIns(3,5)P_2, PtdIns(3)P and PtdIns(3,4,5)P_3. In contrast, the PX domain of p40phox showed specific binding only to PtdIns(3)P. A GST-fusion protein containing the Pleckstrin-homology (PH) of Grp1 (used as a positive control in this assay) showed specific binding only to PtdIns(3,4,5)P_3. This was an expected result on the basis of its known specificity for this phosphoinositide[20,21].

The positions of the two most highly conserved basic residues in PX domains are indicated by an asterisk in the sequence alignment

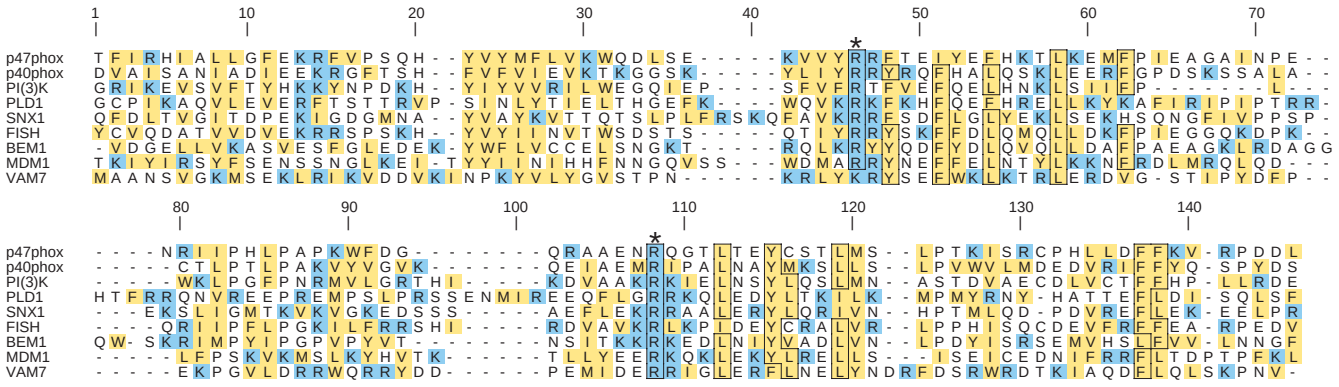

Figure 1 **Sequence alignment of PX domains.** Sequences were aligned using ClustalW and a Gonnet-weight matrix with a gap-opening penalty of 10 and extension penalty of 0.1 for pairwise alignments, and a gap-opening penalty of 10 and extension penalty of 0.2 for multiple alignments. Aliphatic and aromatic residues are shaded yellow; basic residues Arg and Lys are shaded blue. Some of the most highly conserved residues are boxed. The two highly conserved Arg residues are indicated by an asterisk. The accession numbers and corresponding amino acids are: p47phox, P14598, amino acids 4–125; p40phox, Q15080, amino acids 19–140; PI(3)K, O00443, amino acids 1422–1538; Phospholipase D1 (PLD1), Q13393, amino acids 78–213; Sorting Nexin 1 (SNX1), Q13596, amino acids 142–272; FISH, NP_032044, amino acids 4–128; BEM1, P29366, amino acids 278–404; MDM1, Q01846, amino acids 98–222; VAM7, S31263, amino acids 1–125.

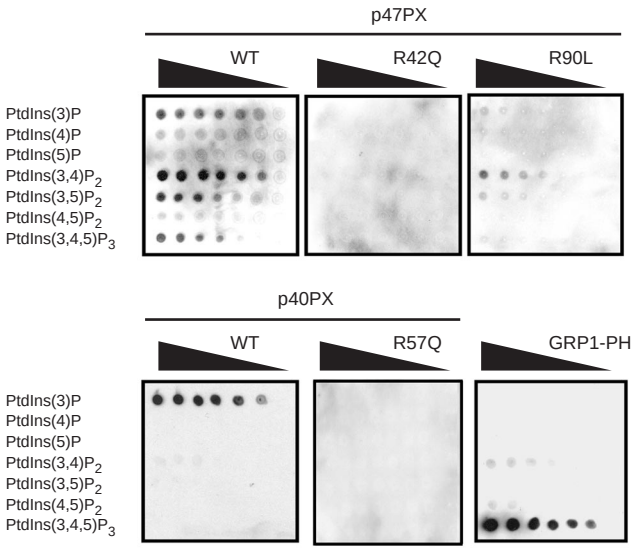

Figure 2 **Phosphoinositide-binding properties of PX domains.** The ability of indicated GST-fusion proteins to bind to a variety of phophoinositides was analysed using a protein–lipid-binding assay. Serial dilutions of indicated phophoinositides (200, 100, 50, 25, 12.5 and 6.25 pmol) were spotted on to Hybond-C extra-membranes, which were then incubated with the purified GST-fusion proteins. The membranes were washed, and the GST-fusion proteins bound to the membrane were detected using an anti-GST antibody. GST–GRP1–PH fusion protein, which is known to bind PtdIns(3,4,5)P_3 (ref. 20), is also shown. A representation of at least three separate experiments is shown. WT, wild type.

(Fig. 1). The first of these, which corresponds to Arg 42 in p47phox, was shown to be mutated to Gln in a subset of patients with the autosomal recessive form of chronic granulomatous disease[22]. The corresponding mutation in the GST–p47PX-domain fusion protein completely eliminated phosphoinositide binding (Fig. 2). A mutation of the analogous residue in the PX domain of p40phox, R57Q, also completely eliminated phosphoinositide binding (Fig. 2). Similarly, mutation of the second conserved Arg residue, R90 in p47phox, to Leu markedly reduced, but did not completely eliminate, phosphoinositide binding (Fig. 2).

The binding of PX domains to phosphoinositides was independently verified using an ultracentrifugation assay for lipid-vesicle binding. As shown in Fig. 3a, the PX domain of p40phox selectively bound to liposomes that contain PtdIns(3)P, but not to liposomes that lack phosphoinositides or contain an alternative monophosphorylated inositol lipid, PtdIns(4)P. The PX domain of p47phox showed preferential binding to liposomes that contain PtdIns(3,4)P_2, particularly at low concentrations of total lipid (Fig. 3b), although binding to liposomes that lack phosphoinositides or contain an alternative di-phosphorylated inositol lipid, PtdIns(4,5)P_2, was observed at higher concentrations of total lipid. This result indicates that the PX domain of p47phox may bind lipids through both specific and non-specific electrostatic interactions. Similar types of specific and non-specific phosphoinositide binding have also been observed for a number of PH domains[21]. No liposome binding was observed for GST alone (data not shown).

Given the high specificity of the PX domain of p40phox for PtdIns(3)P *in vitro*, we examined its ability to bind PtdIns(3)P *in vivo* by fusing this domain to enhanced green-fluorescent protein (EGFP). In NIH3T3 and COS-7 cells, PtdIns(3)P is localized within endosomes[23–25]. In these cell types, p40PX–EGFP localized in a discrete punctate pattern which is consistent with endosomal localization (Fig. 4a, b). This punctate pattern of p40PX–EGFP localization disappeared rapidly when cells were treated with Wortmannin, a specific inhibitor of PI(3)K (Fig. 4a, b; and see Supplementary Information, movie 1). The R57Q mutation that abolished the ability of p40PX to bind to PtdIns(3)P *in vitro* similarly abolished the punctate localization pattern of p40PX–EGFP *in vivo* (Fig. 4c). To confirm that the punctate p40PX–EGFP localization truly reflected endosomes, its location was compared with that of the endogenous EEA1 protein. EEA1 is known to concentrate at early endosomes in part through specific binding of its FYVE domain to PtdIns(3)P[23,26,27]. As shown in Fig. 4d, e, p40PX–EGFP and endogenous EEA1 display significant co-localization. To prove that sites of p40PX localization correspond to sites of endogenous PtdIns(3)P, we used a protein construct consisting of a trimerized EEA1 FYVE domain fused to EGFP, $(FYVE)_3$–EGFP, which is known to specifically localize to sites enriched for PtdIns(3)P *in vivo*[25]. As shown in Fig. 4f, g, p40PX fused to EYFP co-localized with $(FYVE)_3$–EGFP. Taken together, these data indicate that the p40phox PX domain binds to PtdIns(3)P *in vivo*.

Our results show that PX domains are specific phosphoinositide-binding modules, with different PX domains having different phosphoinositide specificity. PX domains now join an expanding

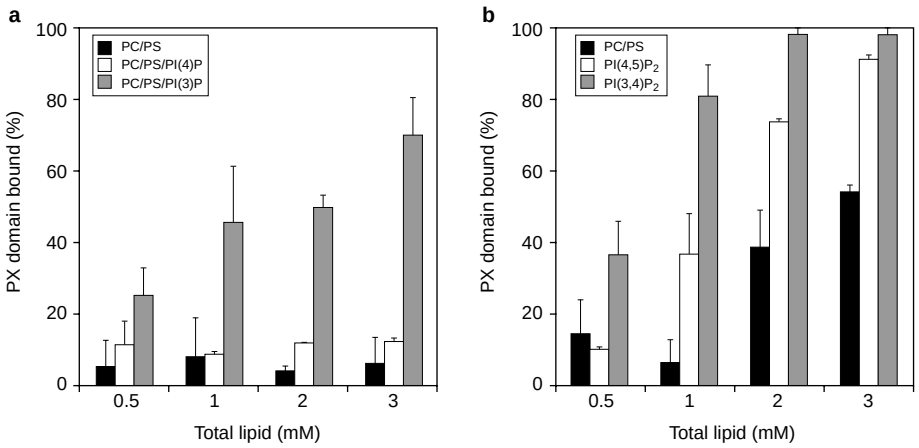

Figure 3 **PX domains bind to lipid vesicles that contain phosphoinositides. a**, **b**, Binding of p40phox (**a**) and p47phox (**b**) PX domain GST-fusion proteins to liposomes that contain PC/PS with or without 3% of the indicated phosphoinositide (PI) was analysed using an ultracentrifugation assay. Error bars represent the s.d. around the mean for three (p40phox) and five (p47phox) independent experiments.

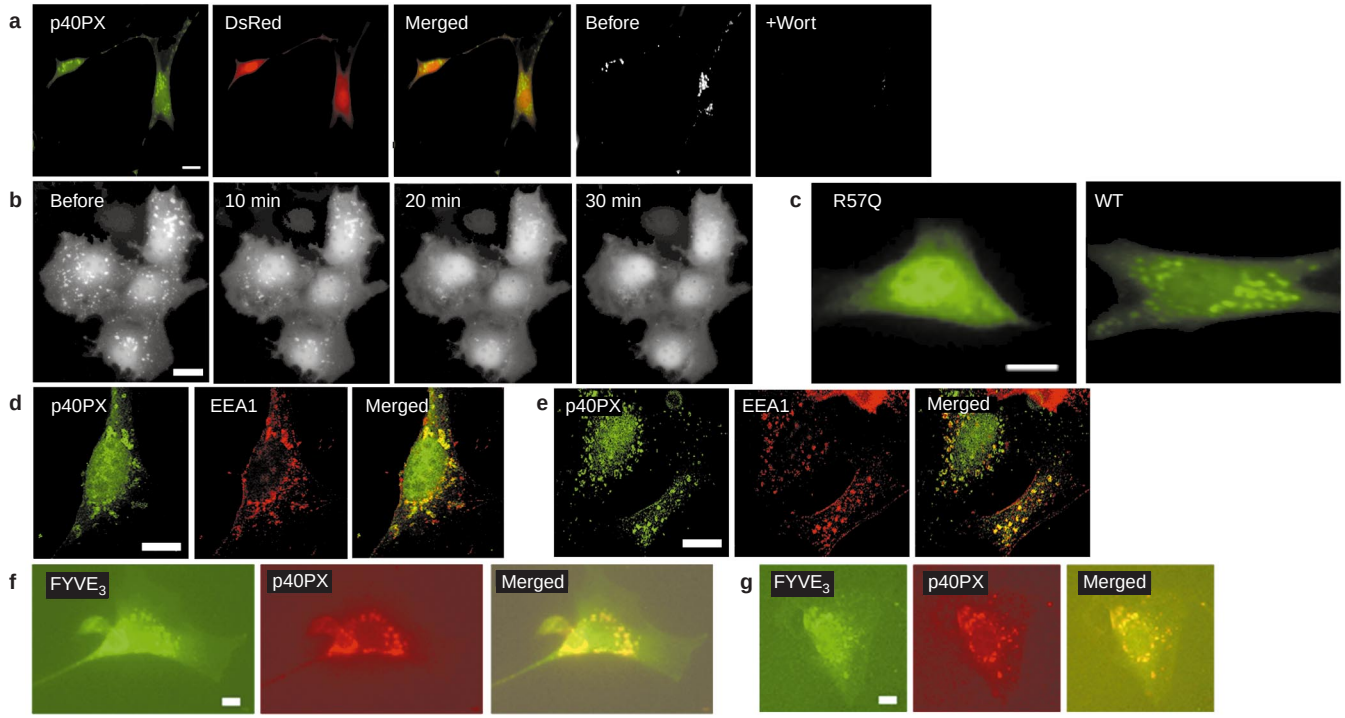

Figure 4 ***In vivo* localization of p40PX–EGFP**. **a**, NIH3T3 cells that express p40PX–EGFP. The fluorescence pattern of p40PX–EGFP, RFP (from DsRed) and a merged image is shown. Subtracted images (GFP minus RFP) controls for non-specific GFP/RFP localization and reveals a discrete punctate cytoplasmic pattern, consistent with localization in vesicles ("before"), which disappears after a 20-min treatment with Wortmannin ("+Wort"). **b**, Time-lapse study of COS-1 cells that express p40PX–EGFP treated with 100 nM Wortmannin. **c**, Punctate localization of p40PX–EGFP is lost by an R57Q mutation that disrupts PtdIns(3)P binding *in vitro*. **d**, **e**, p40PX–EGFP is localized in endosomes. Digital-confocal image of NIH3T3 cells that expressed p40PX–EGFP reveals co-localization of p40PX–EGFP (left panels) and EEA1 (middle panels). **f**, **g**, p40PX–EGFP is localized at sites of PtdIns(3)P accumulation, as indicated by $(FYVE)_3$–EGFP. NIH3T3 cells that express p40PX–EYFP and $(FYVE)_3$–EGFP show co-localization of $(FYVE)_3$–EGFP (left panels) and p40PX–EYFP (middle panels). Scale bar, 10 μm.

family of phosphoinositide-binding modules, which include PH domains, FYVE domains and ENTH domains[18,28–30].

A clear role for PI(3)K in neutrophil function is well established, but the mechanism has been difficult to ascertain. PX domains now provide a direct molecular link between the downstream products of PI(3)K and components of the NADPH oxidase. How the distinct phosphoinositide specificity of the p40phox and p47phox PX domains participates in the assembly of the NADPH oxidase assembly is not yet known. The results are intriguing, however, given the exquisite coordination of phosphoinositol-lipid metabolism observed during formation and internalization of the phagocytic cup in macrophages[31], and the need to assemble the oxidase in neutrophils in

a spatially and temporally regulated manner to avoid inadvertent injury to host tissues. Migration of the cytosolic components of the NADPH oxidase to distinct intracellular membrane compartments is probably controlled, at least in part, through specific PX-domain–phosphoinositide interactions. The inability of the p47phox PX domain of the R42Q mutant to bind to phosphoinositides raises the possibility that this may account for the failure of superoxide generation in this group of patients with chronic granulomatous disease.

PX domains in other proteins are likely to have similar membrane-targeting roles. Proteins of the PX domain-containing nexin family, for example, associate with cellular membranes and interact with a variety of transmembrane receptors, where they have been postulated to have an important role in protein transport among various organelles[3], and in receptor degradation[2]. The yeast vacuolar-sorting proteins Vam7p, Vps5p, Vps17p and Mvp1p all contain PX domains, and mutations in the PX domain of Vam7p inhibit vacuolar transport when combined with a Vam3p temperature-sensitive mutation[6]. Similarly, the protein kinase CISK, implicated in IL-3-dependent cell survival[8], is a structural analogue of the anti-apoptotic protein kinase AKT/PKB, except that the PH domain that precedes the kinase domain in AKT is replaced with a PX domain in CISK. CISK localizes to vesicular compartments within cells, and this localization is strictly dependent upon its PX domain. Thus, it seems likely that PX domains fulfil a general function as phosphoinositide-binding domains in a variety of cellular processes in unicellular and multicellular organisms.

Note added in proof: The interaction of PX domains with phosphoinositides has now been reported in this issue by Cheever *et al. Nature Cell Biol.* **3,** 613–618 (2001), Ellson *et al. Nature Cell Biol.* **3,** 679–682 (2001), and Xu *et al. Nature Cell Biol.* **3,** 658–666 (2001). □

Methods

Materials.

Phosphoinositides were obtained from Cell Signals (Lexington). They were analysed by thin-layer chromatography and they migrated as single products. Fat-free bovine serum albumin (BSA) was obtained from Sigma. A rabbit polyclonal anti-GST antibody was a gift from K. L. Carraway (Beth Israel Deaconess Medical Center, Boston).

Generation of constructs and recombinant proteins.

pGEX-p47 and pGEX-p40 were gifts from A. Hall and F. Wientjes (University College, London). pGEX-GRP1 was a gift from J. K. Klarlund and M. P. Czech (University of Massachusetts Medical School). pGEX-EEA1 was a gift from H. Stenmark (Norwegian Radium Hospital). PX domains from human p47phox (amino acids 2–132) and p40phox (amino acids 1–148) were amplified by polymerase chain reaction (PCR) and were subcloned into pGEX4T1 (Amersham Pharmacia Biotech), which resulted in pGEX-p47PX and pGEX-p40PX, respectively. PX-domain mutants, R42Q and R90L in p47phox, and R57Q in p40phox were generated using the Transformer Site-Directed Mutagenesis Kit (Clontech). The p40PX-domain fragments obtained by PCR were also subcloned into pEGFP-N3 and pEYFP-C1 (Clontech), which generated p40PX–EGFP and p40PX–EYFP. $(FYVE)_3$–EGFP contains three tandem copies of the FYVE domain of EEA1 (residues 1336–1411) subcloned into pEGFP-C1. All constructs were verified by standard DNA sequencing. Plasmid pDsRed1-C1, encoding red-fluorescent protein, was purchased from Clontech.

To isolate recombinant proteins, GST-fusion constructs were expressed in BL-21 cells for 3 h at room temperature, and fusion proteins were purified from bacterial lysates using glutathione–sepharose (Sigma).

Protein–lipid overlay assay.

A protein–lipid overlay assay was performed using GST-fusion proteins as modified from Dowler *et al*[9]. Lipid solution (1 µl) containing 6.25–200 pmol of phosphoinositides dissolved in chloroform/methanol/water (1/2/0.8 volume ration) was spotted onto Hybond-C extra-membranes (Amersham Pharmacia Biotech) and dried at room temperature for 1 h. The membrane was blocked in 3% fat-free BSA in TNE (50 mM Tris (pH 7.5), 150 mM NaCl, 1 mM EDTA) that contained 0.1% Tween-20 at 4 °C overnight. Membranes were incubated at room temperature with the same solution containing 1 µg ml^{-1} of indicated GST-fusion proteins for 1 h, washed five times in TNE containing 0.1% Tween-20, and then incubated for 1 h with an anti-GST antibody (1:1,000 dilution). After washing, the membranes were incubated with horseradish peroxidase-conjugated goat anti-rabbit antibody (Boehringer Mannheim; 1:2,500 dilution) for 1 h at room temperature. The membranes were washed four times at room temperature in TNE containing 0.1% Tween 20, once with Tris-buffered saline (20 mM Tris (pH 7.5), 150 mM NaCl), and signals were detected by enhanced chemiluminescence (NEN Life Science Products).

Liposome-binding assay.

Binding of PX domains to liposomes was performed following the method of Kavran *et al*[21]. Mixtures of 1,2-dibromostearoyl-sn-glycero-3-phosphocholine (PC; Avanti Polar Lipids) and dipalmitoyl phosphatidyl-L-serine (PS; Sigma) (4:1 molar ratio) with and without the indicated phosphatidyl inositides (3% of total lipids) in methanol:chloroform (1:1 volume ratio) containing 0.1% HCl were dried under N_2. After 30 min hydration at room temperature in 10 mM Tris-HCl (pH 7.5) and 75 mM NaCl at a total lipid concentration of 25 mM, unilamellar liposomes were formed by multiple passages (>11) through a Mini-Extruder equipped with a 0.1 µm pore polycarbonate membrane at 45 °C. Purified p40PX–GST or p47PX–GST fusion proteins (10–16 µM) were incubated with liposomes (0–3 mM total lipid) for 1 h at room temperature in a total volume of 100 µl, and the liposomes were pelleted by centrifugation at 300,000 *g* for 1 h. The amount of protein that remained in the supernatant was quantified using the BCA assay (Pierce) and compared with that of a control reaction that contained proteins without lipids.

Microscopy and image collection.

NIH3T3 cells and COS-1 cells were cultured in DMEM supplemented with either 10% calf serum or 10% fetal bovine serum, respectively. Cells grown on glass coverslips were transfected with p40PX–EGFP, p40PX–EYFP, $(FYVE)_3$–EGFP and/or pDsRed-C1 using Lipofectamine (GIBCO-BRL) and observed 24 h after transfection. Wortmannin was used at a final concentration of 100 nM.

Live cells were imaged in a 37 °C microscope chamber using a Nikon-Diaphot-300 microscope which was equipped with a Sensys CCD (charge-coupled device) digital camera (Photometrics), and images were processed using ImageProPlus 4.0 (MediaCybernetics) and Vaytek Imaging Software (Fairfield). Filters used for imaging were as follows (numbers represent filter midpoint/band width in nm): standard EGFP, excitation 475/40, dichroic mirror 460/40, emission 525/40; Texas Red and dsRed, excitation 540/20, dichroic mirror 525/50, emisson 590/long pass; EGFP for use with EYFP, excitation 436/20, dichroic mirror 460/long pass, emission 500/20; EYFP for use with EGFP, excitation 535/30, dichroic mirror 525/50, emission 580/30. All images were captured in a grey scale. Pseudo-colour was added to allow comparisons between images when they were merged.

Immunofluorescence of NIH3T3 cells that transiently expressed p40PX–EGFP was performed by fixing cells with 3.7% paraformaldehyde, permeabilizing with 0.5% NP40, and blocking with 8% BSA in PBS. A mouse monoclonal antibody to EEA1 (BD Signal Transduction) was applied at a concentration of 500 ng ml^{-1} in 1% BSA overnight at 4 °C. Texas Red-conjugated goat anti-mouse secondary antibody (Jackson Immunoresearch) was used at 1 µg ml^{-1} in 1% BSA in PBS for 2 h at room temperature. Extensive washing with PBS was performed between each step and before mounting on slides with Fluoromount G (Southern Biotechnology). Digital confocal images were obtained by imaging adjacent focal planes at 0.3 µm intervals and three adjacent images underwent nearest-neighbour rapid deconvolution using a calculated point-spread function and Vaytek image deconvolution software.

Movies.

NIH3T3 cells that transiently expressed p40PX–EGFP were treated with 100 nM Wortmannin, and images were captured every minute for 30 min; before Wortmannin treatment, images were captured every minute for 8 min. The resultant series of TIFF images (before and after treatment with Wortmannin) was converted to a movie using Quicktime Pro 5.0. Images at the time of Wortmannin treatment (first time point), and 10 and 20 min later are marked as such.

RECEIVED 4 APRIL 2001; REVISED 11 MAY 2001; ACCEPTED 23 MAY 2001;
PUBLISHED 12 JUNE 2001.

1. Ponting, C. P. *Protein Sci.* **5,** 2353–2537 (1996).
2. Kurten, R. C., Cadena, D. L. & Gill, G. N. *Science* **272,** 1008–1010 (1996).
3. Haft, C. R., de la Luz Sierra, M., Barr, V. A., Haft, D. H. & Taylor, S. I. *Mol. Cell Biol.* **18,** 7278–7287 (1998).
4. Phillips, S A, Barr, V A, Haft, D H, Taylor, S I & Haft, C R. *J. Biol. Chem.* 276, 5074–5084 (2001).
5. Horazdovsky, B. F. *et al. Mol. Biol. Cell* **8,** 1529–1541 (1997).
6. Sato, T. K., Darsow, T. & Emr, S. D. *Mol. Cell Biol.* **18,** 5308–5319 (1998).
7. Ekena, K. & Stevens, T. H. *Mol. Cell Biol.* **15,** 1671–1678 (1995).
8. Liu, D., Yang, X. & Songyang, Z. *Curr. Biol.* **10,** 1233–1236 (2000).
9. Babior, B. M. *Blood* **93,** 1464–1476 (1999).
10. Nauseef, W. M. *Proc. Assoc. Am. Physicians* **111,** 373–382 (1999).
11. Wientjes, F. B., Segal, A. W. & Hartwig, J. H. *J. Leukoc. Biol.* **61,** 303–312 (1997).
12. Goldblatt, D. & Thrasher, A. J. *Clin. Exp. Immunol.* **122,** 1–9 (2000).
13. Stephens, L., Jackson, T. & Hawkins, P. T. *J. Biol. Chem.* **268,** 17162–17172 (1993).
14. Arcaro, A. & Wymann, M. P. *Biochem. J.* **296,** 297–301 (1993).
15. Okada, T., Sakuma, L., Fukui, Y., Hazeki, O. & Ui, M. *J. Biol. Chem.* **269,** 3563–3567 (1994).
16. Hirsch, E. *et al. Science* **287,** 1049–1053 (2000).
17. Yaffe, M. B. & Smerdon, S. J. *Structure* **9,** R33–R38 (2001).
18. Fruman, D. A., Rameh, L. E. & Cantley, L. C. *Cell* **97,** 817–820 (1999).
19. Dowler, S. *et al. Biochem. J.* **351,** 19–31 (2000).
20. Klarlund, J. K. *et al. Science* **275,** 1927–1930 (1997).
21. Kavran, J. M. *et al. J. Biol. Chem.* **273,** 30497–30508 (1998).
22. Noack, D. *et al. Blood* **97,** 305–311 (2001).
23. Patki, V. *et al. Proc. Natl Acad. Sci. USA* **94,** 7326–7330 (1997).
24. Lawe, D. C., Patki, V., Heller-Harrison, R., Lambright, D. & Corvera, S. *J. Biol. Chem.* **275,** 3699–3705 (2000).
25. Gillooly, D. J. *et al. EMBO J.* **19,** 4577–4588 (2000).
26. Patki, V., Lawe, D. C., Corvera, S., Virbasius, J. V. & Chawla, A. *Nature* **394,** 433–434 (1998).
27. Stenmark, H., Aasland, R., Toh, B. H. & D'Arrigo, A. *J. Biol. Chem.* **271,** 24048–24054 (1996).
28. Ford, M. G. *et al. Science* **291,** 1051–1055 (2001).
29. Itoh, T. *et al. Science* **291,** 1047–1051 (2001).
30. Mao, Y., Chen, J., Maynard, J. A., Zhang, B. & Quiocho, F. A. *Cell* **104,** 433–440 (2001).
31. Botelho, R. J. *et al. J. Cell Biol.* **151,** 1353–1368 (2000).

ACKNOWLEDGEMENTS

We thank J. Miyagi for technical assistance, S.-Y. Pai for suggesting the R42Q mutation, and members of M.B.Y.'s laboratory for discussions. F.K. was supported by fellowships from the Cell Science Research Foundation and Sankyo Foundation of Life Science. S.J.F. was supported by a Howard Hughes Medical Institute Postdoctoral Fellowship. This work was funded by NIH grants to M.B.Y. and L.C.C, and a Burroughs-Wellcome Career Development Award to M.B.Y.

Correspondence and requests for materials should be addressed to M.B.Y.

Supplementary Information is available on *Nature Cell Biology*'s website (http://cellbio.nature.com).

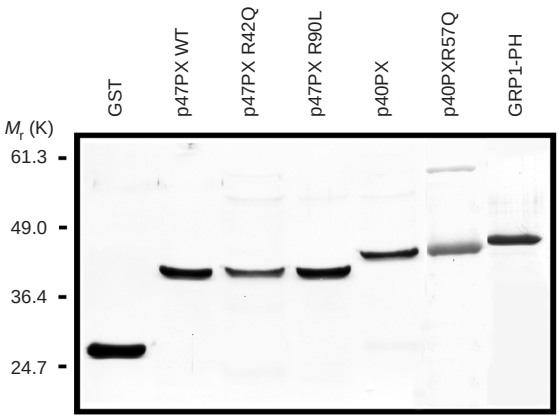

S1 **Expression of GST–fusion proteins of the PX domains from p40phox and p47phox.** The indicated purified GST–fusion of PX-domains (2 μg) were separated by 12% SDS–PAGE and stained with Coomassie blue.

Movie 1 **Loss of endosomal localization of p40PX–EGFP after inhibition of PI(3)K with Wortmannin.** NIH3T3 cells transiently expressing p40PX–EGFP were treated with 100 nM Wortmannin and images were captured every minute for 30 min.